TIME OPTIMAL COORDINATED TURNS USING ENERGY METHODS

by

William Beebee

Measurement Systems Laboratory
Massachusetts Institute of Technology
Cambridge, Massachusetts 02139

Time Optimal Coordinated Turns Using Energy Methods

by

William Beebee

This paper deals with an extension of the energy climb method to solve time-optimal turns for hypersonic rocket-powered aircraft. Specifically, an aircraft makes a coordinated turn to a new heading angle in minimum time, without constraints on the maximum lift. Although there is some change in altitude during the maneuver, it is assumed small enough compared to the horizontal dimensions of the turn that the flight path angle is always small. Because of the hypersonic speed, the aircraft energy is assumed to be almost entirely kinetic, making it a function of velocity only.

To execute the optimal turn, the pilot is given optimal schedules to follow for the roll angle μ and the aircraft altitude, represented by the air density ρ. Thrust and weight are assumed constants. The optimal schedules are determined from the analysis given in this paper. At the start of the turn, the pilot knows his initial energy E_o along with the desired final energy E and azimuth change χ. Figure 3 permits him to estimate which optimal trajectory of χ vs E/E_o contains the above final conditions. The trajectories are characterized by values of the parameter λ. [See equation (20)]. With the value of λ from the desired trajectory and the initial energy known, the pilot refers to Figures 4 and 5. Figure 4 gives the schedule to be followed for roll angle μ as a function of λ , t and E_o. Figure 5 gives the altitude schedule as a function of λ, t and E_o. Figure 6 shows these results applied to a particular problem.

In a recent technical note, Kelly and Edelbaum[1] proposed a formulation of the optimal turn problem which would permit analytic, closed-form integration of the Euler equations. By making additional assumptions listed above it is possible to solve the problem in closed form. The following is a simplified example showing how the technique can be applied.

Assuming a parabolic polar, the drag force on a hypersonic aircraft can be written as

$$D = \frac{1}{2} C_{DO} \rho S V^2 + \frac{2KL^2}{\rho S V^2} \tag{1}$$

where S is a reference area, ρ= air density, V = velocity, L = lift and C_{DO} and K are constants [2]. If the plane possesses a roll angle μ and weight W,

$$W = L\cos\mu \, . \tag{2}$$

This approximation results from assuming the flight path angle to be negligible. The specific energy E ($E = \frac{\text{Kinetic Energy}}{\text{Weight}}$) and the turn angle χ comprise the state and ρ and μ the controls [1]. The following Hamiltonian is to be maximized with respect to ρ and μ.

$$H = \lambda_E \dot{E} + \lambda_\chi \dot{\chi} \tag{3}$$

where λ_E and λ_χ are Lagrange multipliers and $(\cdot)$ denotes differentiation with respect to time. From reference (1),

$$\dot{E} = \frac{(T - D)V}{W} \tag{4}$$

$$\dot{\chi} = \frac{gL}{WV} \sin\mu \, . \tag{5}$$

Using equations (1), (2), (4) and (5) in (3) yields and expanded expression for the Hamiltonian.

$$H = \frac{\lambda_E \left(TV - \frac{C_{DO}\rho S V^3}{2} - \frac{2KW^2 \sec^2\mu}{\rho V S}\right)}{W} + \lambda_\chi \frac{g}{V} \tan\mu \tag{6}$$

The solution for optimum H now proceeds. With respect to ρ,

$$\frac{\partial H}{\partial \rho} = \frac{-C_{DO} S V^3}{2W} \lambda_E + \frac{2KW^2 \sec^2\mu}{W \rho^2 V S} \lambda_E = 0$$

or

$$\rho = \frac{2W \sec\mu}{SV^2} \sqrt{\frac{K}{C_{DO}}} \tag{7}$$

Substituting for ρ into equation (6) yields

$$H = \lambda_E \left(\frac{TV - 2WV\sec\sqrt{KC_{DO}}}{W} \right) + \lambda_\chi \frac{g}{V}\tan\mu \qquad (8)$$

Now, optimize with respect to tan μ.

$$\frac{\partial H}{\partial(\tan\mu)} = -\lambda_E \left(2V\sqrt{C_{DO}K}\,\sin\mu \right) + \lambda_\chi \frac{g}{V} = 0$$

or

$$\sin\mu = \frac{\lambda_\chi}{\lambda_E} \frac{g}{2V^2\sqrt{C_{DO}K}} \qquad (9)$$

Substituting into equation (8), after computing sec μ and tan μ,

$$H = \lambda_E \frac{TV}{W} - \sqrt{\left(2\sqrt{C_{DO}K}\,\lambda_E V \right)^2 - \lambda_\chi^2 \frac{g^2}{V^2}} \qquad (10)$$

This is the equation for optimum H.

The system equations of motion are now used to obtain χ as a function of the specific energy E. Since the plane is moving at hypersonic velocities, making the gravitational potential energy negligible compared to the kinetic energy,

$$E \tilde{=} \frac{1}{2}\frac{V^2}{g}$$

and

$$V \tilde{=} \sqrt{2gE} \qquad (11)$$

decoupling E from the air density ρ. Substituting (11) into equation (10) yields

$$H = \lambda_E \frac{T}{W}\sqrt{2gE} - \sqrt{\lambda_E^2 \left(2\sqrt{C_{DO}K} \right)^2 (2gE) - \lambda_\chi^2 \frac{g}{2E}} \qquad (12)$$

Applying the system equations of motion

$$\frac{\partial H}{\partial \lambda_E} = \dot{E} \qquad (13)$$

$$\frac{\partial H}{\partial \lambda_\chi} = \dot{\chi} \,, \tag{14}$$

it is apparent that

$$\frac{d\chi}{dE} = \frac{\dot{\chi}}{\dot{E}} = \frac{\left(\partial H/\partial \lambda_\chi\right)}{\left(\partial H/\partial \lambda_E\right)} \,. \tag{15}$$

Performing the above differentiations and using (15)

$$\frac{d\chi}{dE} = \frac{\lambda_\chi \frac{g}{2E}}{\lambda_E \frac{T^2}{W^2} 2gE - \frac{HT}{W}\sqrt{2gE} - 2gE\left(2\sqrt{C_{DO}K}\right)^2 \lambda_E} \tag{16}$$

Now, equation (12) is used to obtain λ_E as a function of E and λ_χ.

$$\lambda_E = \frac{1}{\sqrt{2gE}\left(\frac{T^2}{W^2} - 4C_{DO}K\right)} \left[\frac{T}{W} H \pm \sqrt{4H^2 C_{DO}K - \frac{g\lambda_\chi^2}{2E}\left(\frac{T^2}{W^2} - 4C_{DO}K\right)}\right] \tag{17}$$

Substituting equation (17) into (16) and regrouping terms,

$$\frac{d\chi}{dE} = \frac{1}{\sqrt{2C_{DO}K}\sqrt{\frac{1}{4C_{DO}K}\frac{T^2}{W^2} - 1}} \frac{-\left[-\frac{1}{2}\sqrt{\frac{g\lambda_\chi^2}{2H^2}\left(\frac{1}{4C_{DO}K}\frac{T^2}{W^2} - 1\right)\frac{1}{\sqrt{E^3}}}\right]}{\pm\sqrt{1 - \frac{g\lambda_\chi^2}{2H^2 E}\left(\frac{1}{4C_{DO}K}\frac{T^2}{W^2} - 1\right)}} \tag{18}$$

The indefinite integral of $\frac{d\chi}{dE}$ is now seen to be

$$\frac{\pm 1}{2\sqrt{C_{DO}K}\sqrt{\frac{1}{4C_{DO}K}\frac{T^2}{W^2} - 1}} \cos^{-1}\left[\frac{\lambda_\chi}{H}\sqrt{\frac{g}{2E}\left(\frac{1}{4C_{DO}K}\frac{T^2}{W^2} - 1\right)}\right], \tag{19}$$

where the property λ_χ = const. has been used [1]. The expression in (19) can be rewritten in terms of the ratio (specific energy E/ initial specific energy E_o) and other terms:

$$\frac{\pm\left(\frac{L}{D}\right)_{max}}{\sqrt{\left(\frac{T}{W}\right)^2 \left(\frac{L}{D}\right)^2_{max} - 1}} \cos^{-1}\left(\frac{1}{\sqrt{\eta}}\lambda\right) \tag{20}$$

where $\eta \equiv E/E_o$,

$$\lambda \equiv \frac{\lambda_\chi}{H}\sqrt{\frac{g}{2E_o}\left(\left(\frac{T}{W}\right)^2 \left(\frac{L}{D}\right)^2_{max} - 1\right)}$$

and $\left(\frac{L}{D}\right)_{max} \equiv \frac{1}{2\sqrt{C_{DO}K}}$. From this information it is apparent that

$$\chi = \int_{E_o}^{E} \left(\frac{d\chi}{dE}\right) dE = \frac{\left(\frac{L}{D}\right)_{max}}{\sqrt{\left(\frac{T}{W}\right)^2 \left(\frac{L}{D}\right)^2_{max} - 1}} \left[\pm \cos^{-1}\left(\frac{1}{\sqrt{\eta}}\lambda\right)\right] + \text{constant} \tag{21}$$

Evaluating the definite integral gives a series of curve pairs, plotted for various λ in figure 1. Note that when $\lambda = 1$, the curve pair merges.

Now, we obtain t as a function of E. Equation (13) is inverted to obtain

$$\frac{dt}{dE} = \left(\frac{\partial H}{\partial \lambda_E}\right)^{-1} \tag{22}$$

Performing the $\frac{\partial H}{\partial \lambda_E}$ differentiation,

$$\frac{dE}{dt} = \frac{\lambda_E \left(\left(\frac{T}{W}\right)^2 V^2 - V^2 \left(2\sqrt{C_{DO}K}\right)^2\right) - H \frac{T}{W} V}{\lambda_E \frac{T}{W} V - H} \tag{23}$$

We now combine equation (11) and (17) with (23) and solve for $\frac{dt}{dE}$

$$\frac{dt}{dE} = \frac{\left(\frac{L}{D}\right)^2_{max}}{\left(\left(\frac{T}{W}\right)^2 \left(\frac{L}{D}\right)^2_{max} - 1\right)\sqrt{2gE_0}} \left\{ \frac{\left(\frac{T}{W}\right)}{\sqrt{E/E_o}} + \frac{\left(\frac{D}{L}\right)_{min}}{\pm\sqrt{E/E_o - \lambda^2}} \right\} \quad (24)$$

using the definitions of $\left(\frac{L}{D}\right)_{max}$ and λ from equation (20). The indefinite integral of $\frac{dt}{dE}$ is found with little effort, and, substituting η for E/E_o, we obtain

$$t = \int_{E_o}^{E} \frac{dt}{dE}\, dE = \frac{\left(\frac{L}{D}\right)^2_{max}}{\left(\left(\frac{T}{W}\right)^2 \left(\frac{L}{D}\right)^2_{max} - 1\right)} \sqrt{\frac{2E_e}{g}} \left\{ \frac{T}{W}\sqrt{\eta} \pm \left(\frac{D}{L}\right)_{min} \sqrt{\eta - \lambda^2} \right\} + \text{constant} \quad (25)$$

Two positive integrals result for each value of λ in equation (25). They are shown in figure 2. As in figure 1, letting $\lambda = 1$ gives only one curve. Figure 3 shows χ vs. E/E_o with normalized time cross-plotted on the same graph.

In order to obtain the time-optimal schedules for μ and ρ, we set H = 1 by convention [see ref. (3)]. From equation (20), it is apparent that

$$\lambda_x = \lambda \Big/ \sqrt{\frac{g}{2E_o}\left(\left(\frac{T}{W}\right)^2 \left(\frac{L}{D}\right)^2_{max} - 1\right)} \quad (26)$$

Equation (9) can be solved for sec μ to yield

$$\sec \mu = \frac{\lambda_E V^2}{\sqrt{\lambda_E^2 V^4 - g^2 \lambda_x^2 \left(\frac{L}{D}\right)^2_{max}}} \quad (27)$$

After extensive manipulation using equations (11),(17),(26) and (27), we obtain

$$\mu = \sec^{-1}\left\{\frac{\left(\frac{T}{W}\right)\left(\frac{L}{D}\right)_{max} \pm \sqrt{1 - \lambda^2/\eta}}{\pm\left(\frac{T}{W}\right)\left(\frac{L}{D}\right)_{max}\sqrt{1 - \lambda^2/\eta} + 1}\right\} \tag{28}$$

where the $\pm$ sign follows the $\pm$ in equation (25). Thus, two distinct optimal bank angle trajectories result for each value of λ in figure 4; they correspond to the two χ vs η trajectories for each value of λ in figure 3. The corresponding altitude schedule for

$$\text{Normalized } \rho \text{ vs } \sqrt{\frac{g}{2E_o}}\, t$$

is given in figure 5.

Some interesting phenomena are seen in Figures 3-6. Note that, according to Figure 3, λ cannot be smaller than .6 for the backward bending curves on the left of the graph. These curves result from assuming the (-) signs in equations (20) and (24). The reason for this constraint can be seen from equation (24). If

$$\lambda < \sqrt{1 - \left(\frac{W}{T}\right)^2 \left(\frac{D}{L}\right)^2_{min}},$$

the derivative $\frac{dt}{dE}$ is positive for certain values of η less than 1. Performing an integration of $\frac{dt}{dE}$ in the negative direction (which yields the backward bending curves seen above) causes t to be negative. Since this is an impossible result, we have to obey the above λ constraint. Figure 4 gives a better physical picture of this situation. When the critical value of λ is assumed, the aircraft is required to bank at a 90° (1.56 rad) roll angle. From equations (2) and (5), the lift goes to infinity and $\dot{\chi}$ goes to infinity when 90° roll is executed. This causes an impulsive drop in energy because the drag is proportional to the square of the lift [equation (1)]. In figure 3 there is a separate family of backwards bending curves for the critical λ value. Each curve starts out with a different initial energy, each value less than E_0 because of the above impulsive energy change. As the initial energy approaches zero, the time needed to achieve any desired azimuth change approaches zero. In the limit the infinite drag causes an instantaneous loss of all kinetic energy (forward motion stops) and any desired azimuth change occurs in zero time.

References

1. Kelly, Henry J., and Edelbaum, Theodore N., "Energy Climbs, Energy turns and Asymptotic Expansions", Analytical Mechanics Associates memo under NASA/ERC contract NAS 12-757.

2. Miele, A., Flight Mechanics, Vol. 1, Chapter 9, Reading: Addison Wesley Publishing Company, Inc. 1962.

3. Pontryagin, et. al., Mathematical Theory of Optimal Processes, New York: John Wiley, Publishers, 1962.

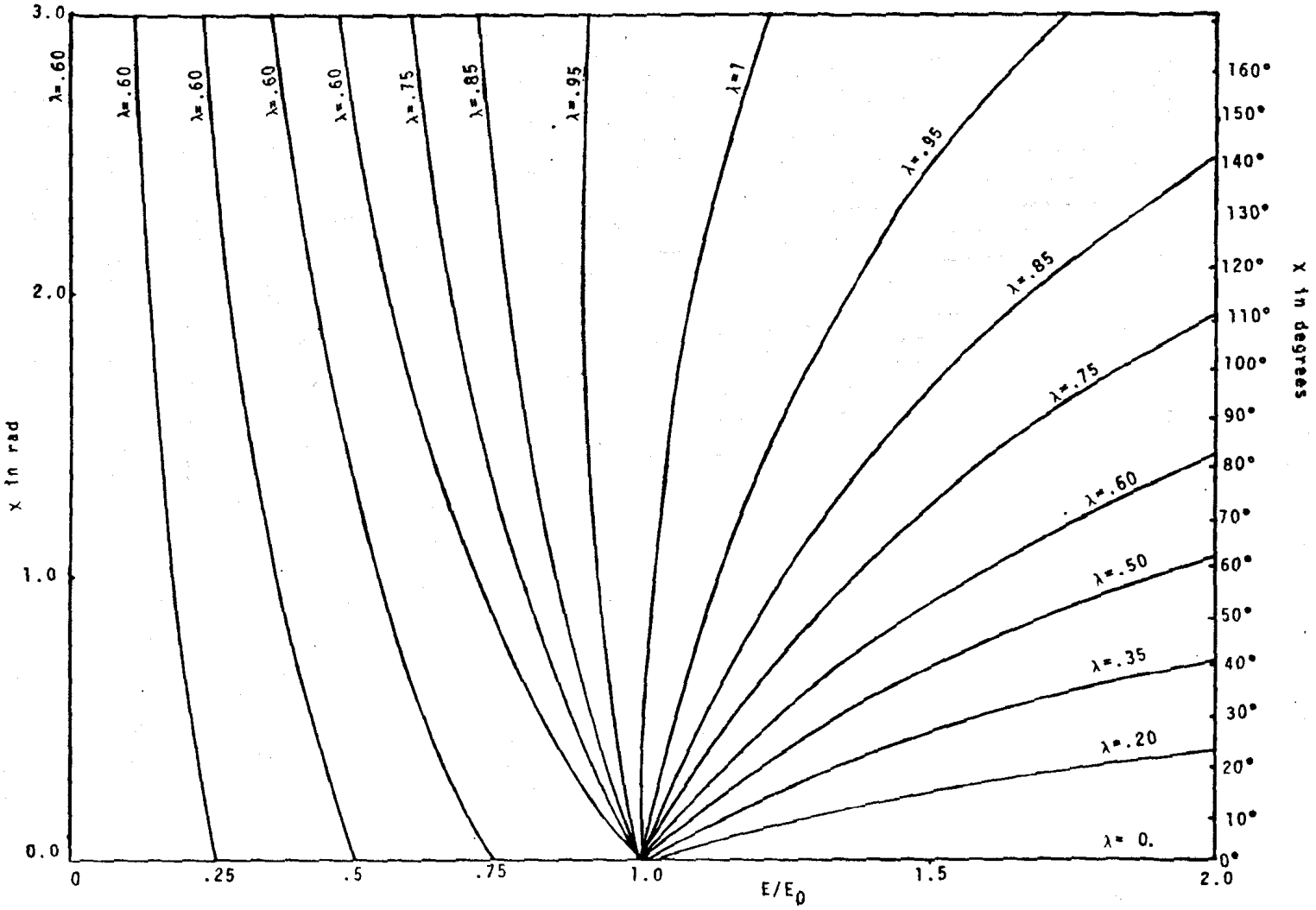

FIGURE 1: χ vs. E/E_0 for Various λ Values

NOTE: $\frac{T}{W} = .25$, $\left(\frac{L}{D}\right)_{MAX} = 5$

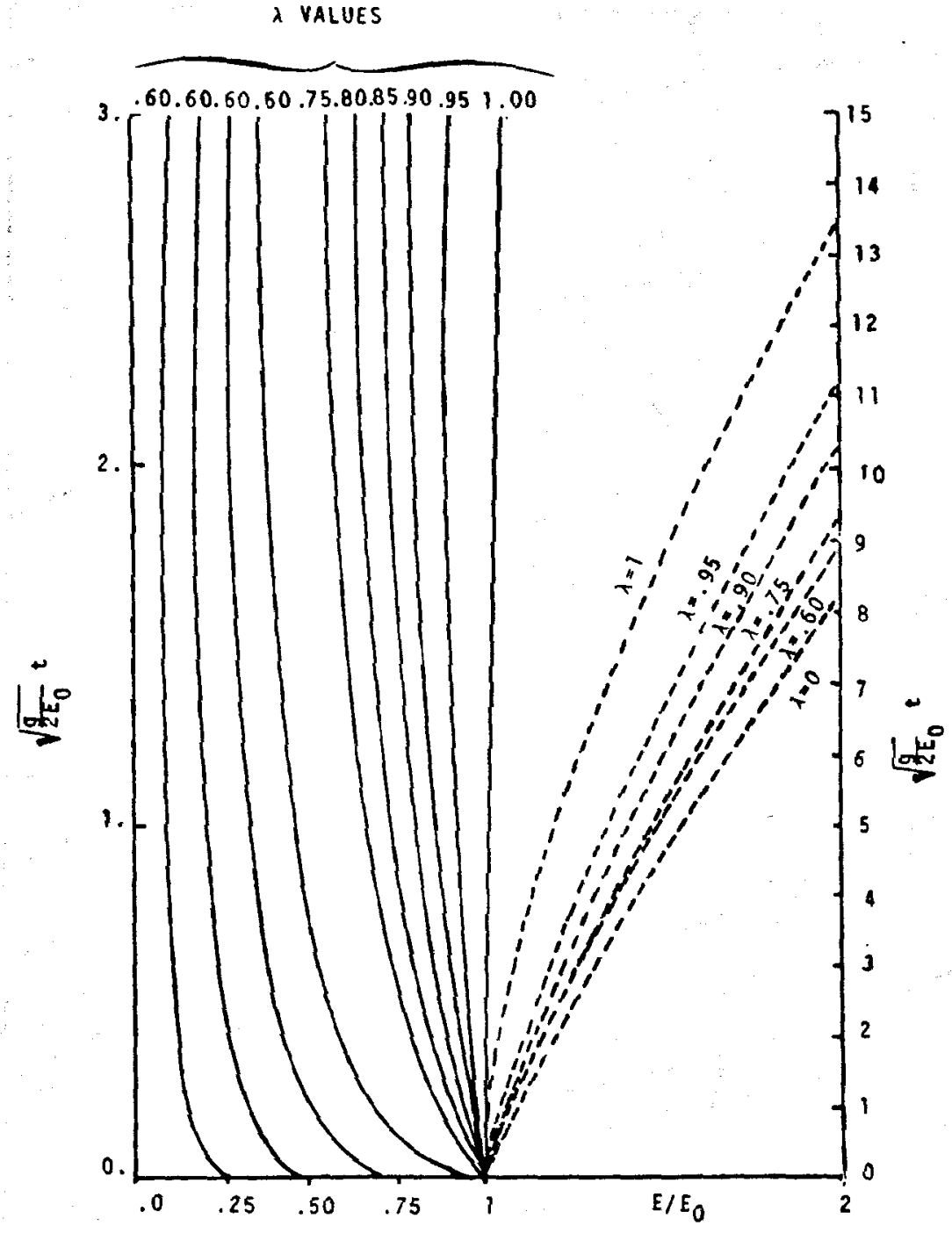

FIGURE 2: $\sqrt{\frac{q}{2E_0}}\ t$ vs. E/E_0 on Two Scales

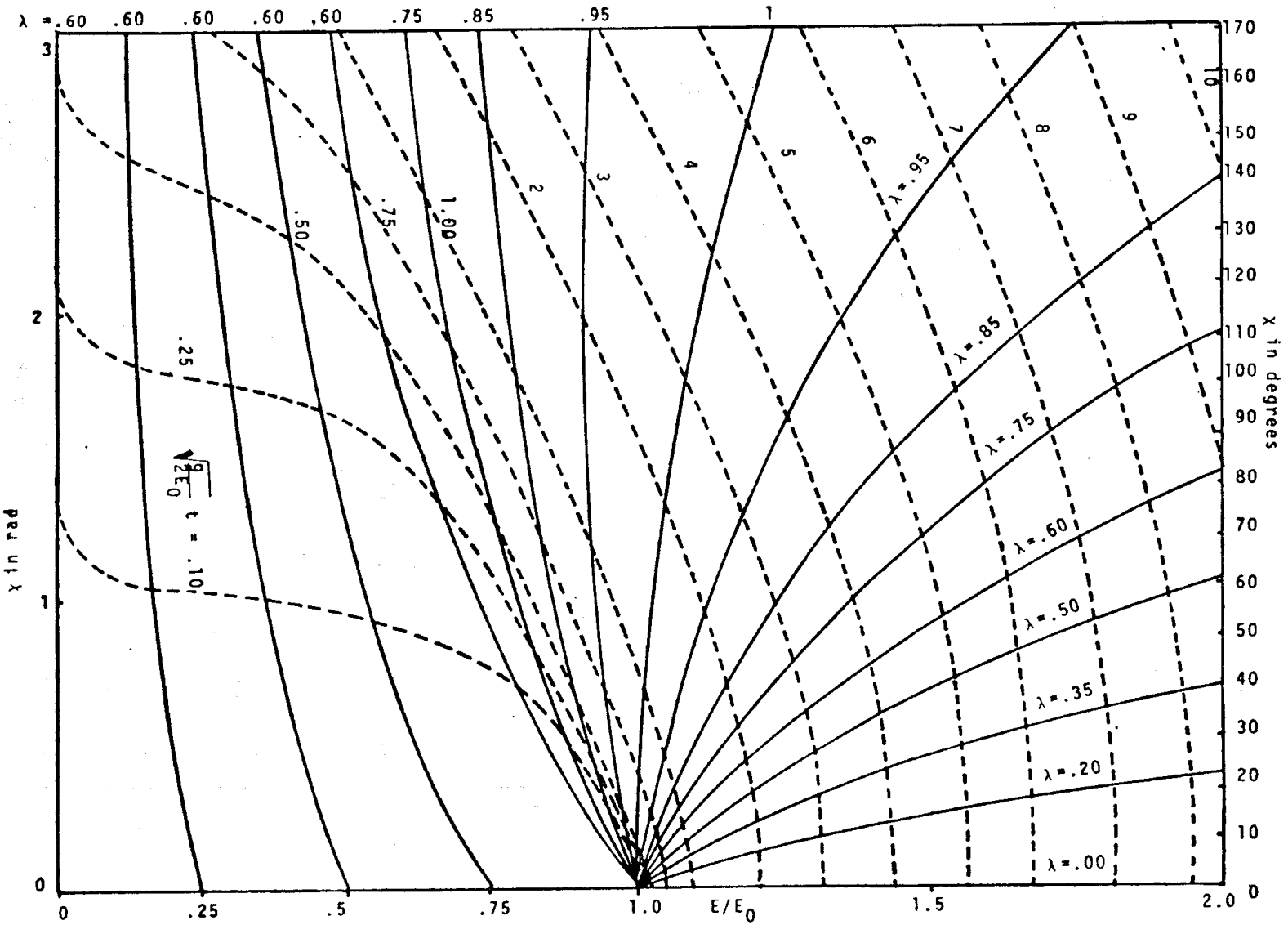

FIGURE 3: X vs. E/E_0 With Time Cross-plot

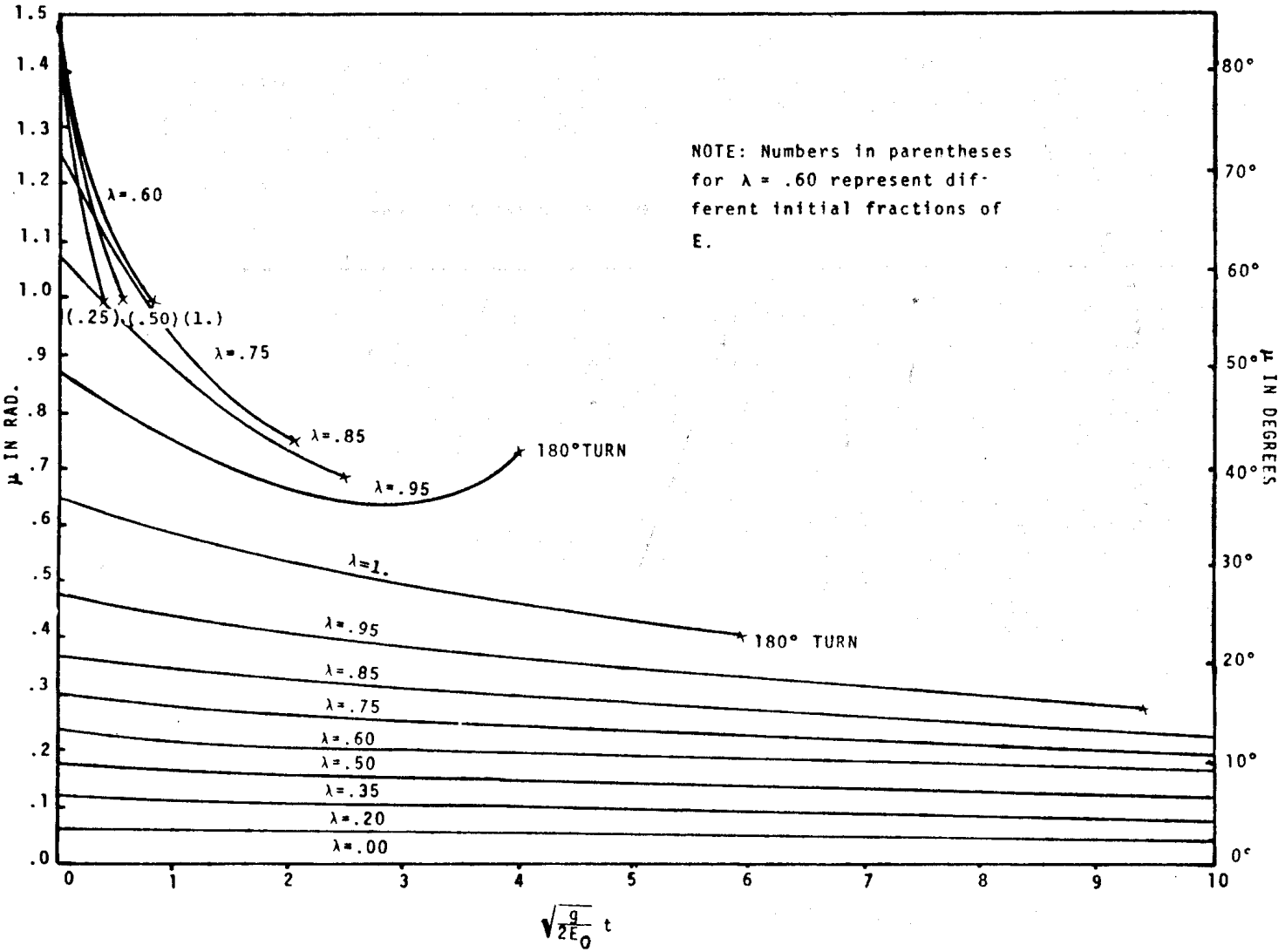

FIGURE 4. ROLL ANGLE SCHEDULES FOR TIME-OPTIMAL TURNS OF FIG. 3.

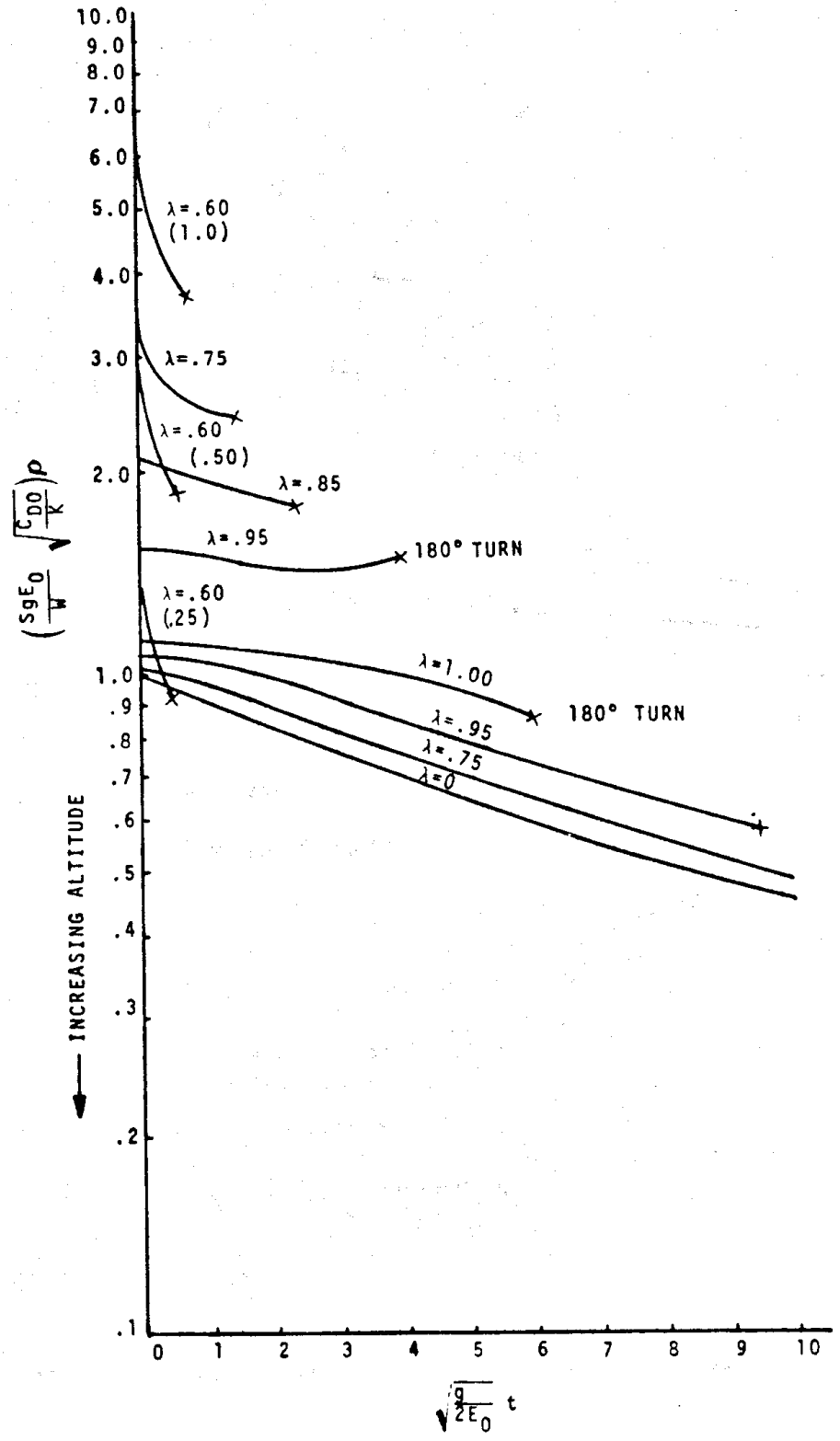

FIGURE 5: NORMALIZED ALTITUDE VS. NORMALIZED TIME FOR λ VALUES IN PREVIOUS FIGURES

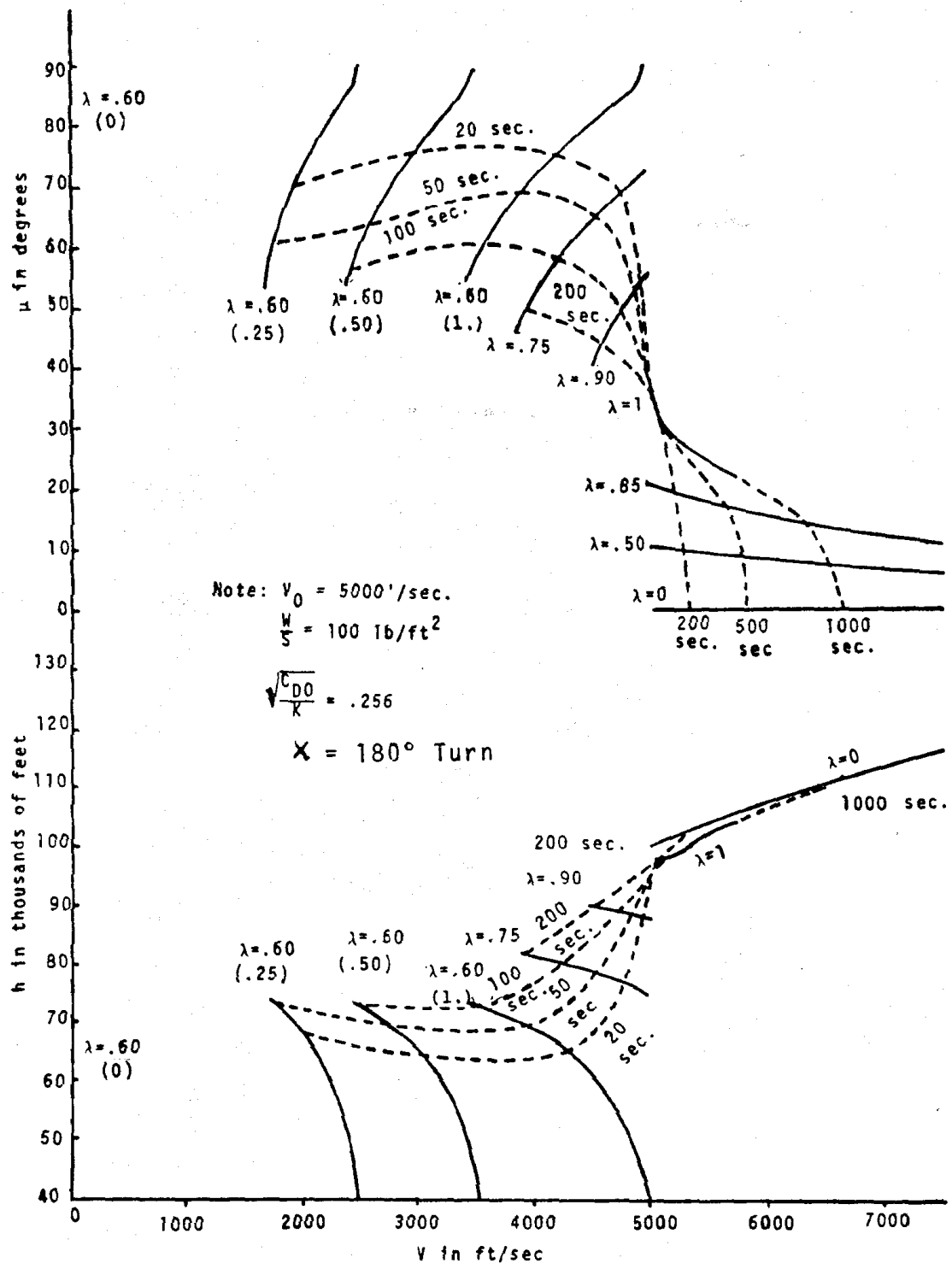

Figure 6: Performance Curves for Particular Parameter Values